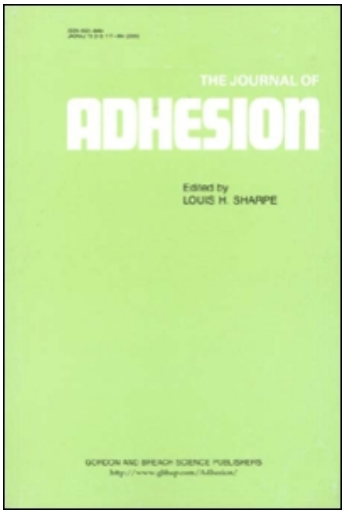

The Journal of Adhesion

Publication details, including instructions for authors and subscription information:
http://www.informaworld.com/smpp/title~content=t713453635

Optimum Polymer - Solid Interface Design for Adhesion Strength: Carboxylation of Polybutadiene and Mixed Silanes Surface Modification of Aluminum Oxide

Ilsoon Lee[a]; Richard P. Wool[a]

[a] Department of Chemical Engineering, University of Delaware, Newark, DE, USA

To cite this Article Lee, Ilsoon and Wool, Richard P.(2001) 'Optimum Polymer - Solid Interface Design for Adhesion Strength: Carboxylation of Polybutadiene and Mixed Silanes Surface Modification of Aluminum Oxide', The Journal of Adhesion, 75: 3, 299 — 324

To link to this Article: DOI: 10.1080/00218460108029606

URL: http://dx.doi.org/10.1080/00218460108029606

J. Adhesion, 2001, Vol. 75, pp. 299–324
Reprints available directly from the publisher
Photocopying permitted by license only

Optimum Polymer – Solid Interface Design for Adhesion Strength: Carboxylation of Polybutadiene and Mixed Silanes Surface Modification of Aluminum Oxide*

ILSOON LEE and RICHARD P. WOOL†

Department of Chemical Engineering, University of Delaware, Newark, DE 19716, USA

(Received 25 April 2000; In final form 4 October 2000)

To understand the optimum design of polymer–solid interfaces for adhesion strength, model polymer–solid interfaces of carboxylated polybutadiene (cPBD) adhered to mixed silane modified Al_2O_3 surfaces were examined. The cPBD, having various —COOH sticker group concentration $\phi(X)$ ($0 \sim 10$ mol %), was synthesized through high-pressure carboxylation of PBD, while Al_2O_3 surfaces were modified to have various $—NH_2$ density, $\phi(Y)$ ($0 \sim 100$ mol %), using self-assembly of mixed amine- and methyl-terminated silanes. The coadsorption kinetic model of the two silanes was analyzed through X-ray photoelectron spectroscopy (XPS), atomic force microscope (AFM), and dynamic contact angle (DCA), which gave the capability of controlling the receptor concentration of aluminum oxide surfaces. The polymer surface chain responses after exposure to various media were understood by measuring contact angle changes of various probe liquids. T-peel tests of the model polymer–solid interfaces, as a function of time and sticker and receptor group concentrations showed much longer time dependence than the characteristic time of a bulk polymer chain. Additionally, the classical equation of interface failure was re-examined to see the effects of deformation rate, annealing temperature, and annealing time. A simple scaling analysis of free energy of an adsorbed polymer on a solid surface was extended to predict the adhesion potential of the model polymer–solid interfaces. From the experiments and theory of adhesive *vs.* cohesive failure, it was found that there existed an optimum product value $r^* = \phi(X)\phi(Y)\chi$ of sticker concentration $\phi(X)$, receptor concentration $\phi(Y)$, and their interaction strength χ,

---

* Presented at the 23rd Annual Meeting of The Adhesion Society, Inc., Myrtle Beach, South Carolina, USA, February 20–23, 2000.

† Corresponding author. Tel.: 302-831-3312, Fax: 302-831-1048, e-mail: wool@ccm.udel.edu

which was approximately 150 cal/mol for this polymer–solid interface. Below or above this optimum product value r^*, the fracture energy of polymer–solid interfaces, G_{IC}, was less than its optimal value, G_{Ic}^*.

Keywords: Adhesion; Optimum design; Carboxylated polybutadiene-aluminum interfaces; T-peel tests; Self-assembled silanes; Sticker groups; Contact angle; AFM analysis; XPS analysis; SEM analysis

1. INTRODUCTION

The interfaces between hydrophobic polymers, such as polyethylene (PE), polypropylene (PP), polybutadiene (PB), and polystyrene (PS), and hydrophilic solid surfaces, such as metal, glass, and wood, are extremely weak. This is because there are no specific interactions except for dispersive forces by van der Waals interactions between polymers of low surface energy and solid surfaces of high surface energy. The van der Waals interactions at the polymer–solid interfaces are not enough to make the failure occur cohesively in polymer layers, since the polymer chains are entangled with van der Waals interactions and some other interactions which depend on the molecular components of polymers. To improve polymer adhesion on high energetic surfaces, functional groups (sticker groups) can be added to the polymer. For example, monomers of PE, PP, PB, and PS are copolymerized with sticker monomers, such as maleic anhydride, acrylic acid, and sulfonic acid. In addition, surfaces of PE, PP, PB, and PS are chemically modified to have such stickers. These sticker groups can chemically interact with receptor groups placed on the solid surface. Specific sticker–receptor interactions which need to be stronger than van der Waals interactions, such as hydrogen bonds, acid–base interactions, or covalent bonds at the polymer–solid interfaces are required to make strong polymer–solid interfaces, which make the failure occur in polymer layers, resulting in improving the adhesion of polymers [1–4]. As an example of the improvement of polymer adhesion, the poly(ethylene-co-acrylic acid) (PEAA)–aluminum (Al) interface is much stronger than polyethylene–aluminum interface [5].

For these modifications, giving polymers sticker groups, many industrial techniques are used. Plasma, laser, corona, UV, and ozone treatment, as well as copolymerization and chemical modification were developed for such purposes [6–8]. The concentration and type of sticker groups along the polymer chain have been the critical issue of

designing optimum polymer–solid interfaces [1–8]. Recently, because of technical limitation or the sudden change of polymer characteristics by the modification, it becomes more desirable to modify solid surfaces and to control the concentration and the type of receptors as well as modifying polymers to control the stickers. Understanding the interplay between stickers and receptors on a molecular level is crucial for an optimum design of strong polymer–solid interfaces. However, most research has been limited to determining the effect of the extent of modification on the improvement in material properties.

The interplay of polymer sticker groups ($-X$) and substrate receptor groups ($-Y$) is the main factor controlling the structure and the strength of the polymer–solid interface. In this work, the problem was defined as the $X-Y$ problem at the polymer–solid interface, as shown in Figure 1. Because a polymer and a solid surface have multiple interacting sites, the interplay depends on sticker group concentration, receptor group concentration, and the sticker and receptor pairs. In regard to the X problem of polymer adhesion, various polymer-substrate systems have been studied [1–7, 9, 10]. Several copolymer-substrate systems have shown that there existed an optimum behavior of fracture energy as a function of sticker group concentration, as shown in Figure 2. The optimum concentration varied depending on stickers and receptors. It was qualitatively explained [10] that the decreasing fracture energy after the optimum concentration was due to the excessive interfacial bonds, which caused the interfacial chains to entangle with themselves rather than with the chains in the bulk.

This optimum behavior in polymer adhesion appears to be universal because other simple adhesion systems have also shown that optimum adhesion behavior. The adhesion between a pseudo-brush and a polymer melt [11] and the adhesion between immiscible polymer–polymer

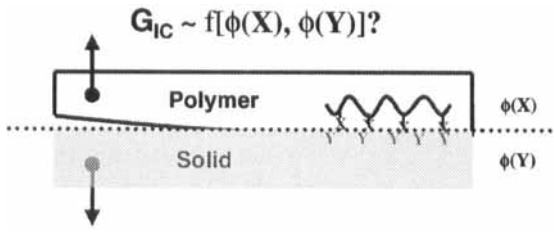

FIGURE 1 Schematic representation of the $X-Y$ problem at the polymer–solid interface.

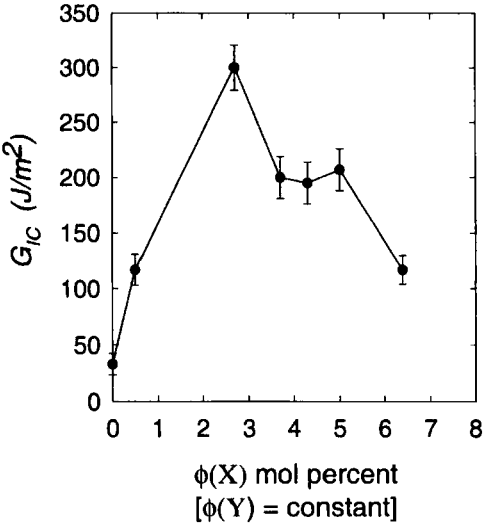

FIGURE 2 Polymer sticker concentration effect on the fracture energy of cPBD–Al interfaces at 1000 minutes annealing time in which the receptor concentration were the same (100 mole % —OH) and the peeling rate was 30 mm/min [10].

interfaces reinforced by block copolymers [12] are such systems showing an optimum fracture energy as a function of areal density. For polymer brushes, the reason for such optimum behavior was explained by the concentration-dependent interdigitation between brushes and polymer melts [11]; at low concentration, the interdigitation was high due to the random walk nature of the tethered chains, while, at high concentrations, the chains formed an organized brush with diminished interdigitation with the melt chains. Additionally, Inagaki *et al.* showed an optimum behavior in the peel strength of copper-perfluoroalkyl vinyl ether (PFA) as a function of remote hydrogen plasma treatment time [8]. All of these results indicate that the interface can be optimized through the selection of the molecular parameters that are responsible for the interface structure and strength. Phenomenologically, all of the systems above are the same. This is because the chain conformation of the polymer brushes on the solid surfaces and an adsorbed polymer chain from the polymer melt onto a plane surface can be analyzed in a similar way. The layer of adsorbed chain on a solid surface can be visualized as a succession of loops and tails. With the help of Guiselin's approach, each loop made

of $2n$ monomers can be considered as two pseudo-tails of n monomers [13], so the two systems are basically the same. The optimum value of the sticker concentration, $\phi(X)$, however, should depend on the receptor concentration, $\phi(Y)$; $\phi(Y)$ strongly affects the restructuring process of an interfacial polymer chain, which determines the adhesion kinetics. Typically, most polymer adhesion studies have been discussed after short annealing times based on the time scale of a bulk chain, such as terminal relaxation time, reptation time, and self-diffusion time. The restructuring time of a chain near an interface could be much longer than the relaxation time of a free bulk chain, up to 10^5 times, depending on the enthalpic driving forces between a polymer and a solid surface [14]. An enthalpic driving force between polymer and surface can decrease the gap between the two characteristic times of a bulk chain and a tethered chain on a solid surface. Generally, different treatment methods have been compared with the surface energy relating to thermodynamic work of adhesion. Fowkes and Mostafa related the work of adhesion to the enthalpy of sticker–receptor interactions [15]. Their relation predicted that the work of adhesion increases with increasing number of sticker–receptor pairs per unit area of interface. However, this prediction cannot explain the optimum fracture energy behavior observed in many polymer–solid interface systems [1, 8–10].

In this work, polybutadiene was chemically modified to add —COOH sticker ($-X$) groups and aluminum oxide surfaces were treated with silanes to add —NH_2 receptor ($-Y$) groups. From these modifications weak PBD–Al interfaces were changed to strong cPBD-AlS (S = silane) interfaces. The fracture energy of these interfaces showed an optimum behavior as a function of sticker and receptor concentrations. Here the design strategy for an optimum polymer–solid interface is generalized, which is a function of sticker concentration, receptor concentration, and sticker–receptor interaction strength.

2. EXPERIMENTAL

2.1. Carboxylation of Polybutadiene

Polybutadiene (Firestone Diene 35A with $M_n = 98{,}000$, $M_w = 180{,}000$ and 10 mol % vinyl groups) was chemically modified using a

high-pressure carboxylation reaction to have a small amount of carboxylic acid sticker groups, —COOH [9,16]. The extent of carboxylation of cPBD, ϕ_X(COOH), was determined *via* FTIR using a KBr liquid cell and a standard calibration curve prepared using di-carboxy terminated polybutadiene (dPBD, $M_n = 4{,}200$). The glass transition temperature of cPBD was approximately $-90°$ C, and the distribution of —COOH was random along the polymer chain [16]. No significant chain scission or cross-linking was detected during the reaction [16].

2.2. Mixed Silane Modification of Aluminum Oxide Surfaces

The model substrates with varying density of $-NH_2$ (0–100 mol %) on Al_2O_3 were prepared using a self-assembly of mixed amine-terminated silanes (AS; γ-aminopropyltrimethoxy silane; $H_2NCH_2CH_2CH_2Si(OMe)_3$) and methyl-terminated silanes (MS; *n*-propyltrimethoxy silane; $CH_3CH_2CH_2Si(OMe)_3$). The details of silane self-assembly are well known [9,17]. The Al foil, purchased from Shim Stock Inc., was first pretreated overnight at 300°C in an oven to ensure the formation of a stable layer of native oxide. The thickness of the Al foil was 25 μm, and the roughness average (RA) was determined to be about 0.5 μm using a scanning white light interferometer (SWLI). The total combined concentrations of AS and MS in the mixed silane water solutions were 50 mM (ca. 0.8 wt %). The pH of the solutions was maintained at 4.5 for all solution concentrations using acetic acid. To apply silane coatings, samples were dipped in solution for 5 min. The silane-treated substrates were rinsed thoroughly with distilled water to prepare monolayer-like silane coatings. After rinsing, the monolayer-like silane coatings were dried at room temperature for 1 hour and then cured in an oven under N_2 purging at 115°C for 30 minutes. The surface composition was determined by X-ray photoelectron spectroscopy (XPS). In addition, an atomic force microscope (AFM) and a dynamic contact angle (DCA) analyzer were used to characterize the model substrates further. The thickness of the silane coatings was uniform regardless of surface concentrations. However, it was not clear whether the model surfaces were monolayers, so they will be called "monolayer-like silane coatings" in this paper.

2.3. Interfacial Fracture Energy

The fracture energy, G_{IC}, of the AlS-cPBD-AlS interfaces was evaluated using a T-peel test, as illustrated in Figure 3. A layer of cPBD was uniformly cast from 2 wt % solution in toluene onto the substrate. The thickness of the cPBD was estimated to be approximately 16 μm, based on volume of solution cast, surface area covered, and weight gain. After the toluene was evaporated under vacuum for 15 min, another substrate was used to form AlS-cPBD-AlS sandwich structures. After being pressed together to ensure good contact, the AlS-cPBD-AlS structure was annealed under 4 kPa pressure at room temperature for different times. The jointed sandwich samples were cut into specimens with dimensions of 60 mm in length and 10 mm in width. The fracture energy, G_{IC}, was obtained from the average of three tests per material and is given by

$$G_{IC} = \frac{2P}{b} \tag{1}$$

where P is the peel load and b is the width of the test sample.

2.4. Contact Angle Analysis

The surface wetting properties of the monolayer-like silane coatings on Al_2O_3 and the cPBD-coated glass cover slides were investigated with a

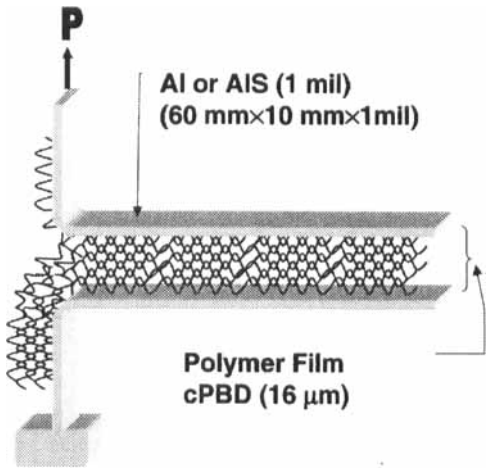

FIGURE 3 Schematic representation of T-peel test.

CAHN DCA analyzer using a Wilhelmy plate technique. Hexadecane, water (HPLC grade), and methylene iodide were used as probing liquids. Thicker aluminum foil (Shim Stock Inc., thickness of 250 μm) was used for monolayer-like silane coatings on Al_2O_3. The thick Al foils were cut into small pieces (24 mm × 50 mm × 0.25 mm). The Al pieces were coated with silanes using the preparation methods described in Section 2.2. Cover glass slides (Fisher, 24 mm × 50 mm × 1 mm) were used for the cPBD-coated glass cover slides. The cover glass slides were immersed in a Nochromix-sulfuric acid solution for 24 h, rinsed extensively with purified water (Fisher, HPLC grade), and then dried overnight in a vacuum oven at 100°C. The clean glass slides were dipped in dilute cPBD-toluene solution (1 wt %) for 24 h and then dried in air and under vacuum for 30 min and 1 h, respectively. The plate-moving speed was 22 μm/s.

2.5. AFM Analysis

The silane coverage and two-dimensional distribution of AS and MS in the mixed monolayer-like silane coatings on Al_2O_3 were explored with an Atomic Force Microscope (AFM) in TappingMode™. A silicon probe with dimension of 125 × 3 × 1 μm and a tip radius of 5–10 nm was oscillated at its mode-1 resonance frequency and setpoint voltage between 50 and 55% of the free vibrational amplitude in air. The difference between the setpoint and the free amplitude was directly related to the amount of force applied to the surface during the imaging. To verify surface structures observed with AFM, untreated Al_2O_3 surfaces were also imaged. The AFM images of intermediate densities, between $\phi_Y = 1$ and $\phi_Y = 0$, appeared to be different from those of $\phi_Y = 1$, $\phi_Y = 0$, and the pure Al_2O_3. However, the images were not clear enough to distinguish the intermediate densities [18].

2.6. XPS Analysis

The surface composition of the model substrates was analyzed by a Leybold-Heraeus XPS. This system has a monochromatic Mg Kα X-ray source ($h\nu = 1253.6$ eV). The pressure in the sample chamber was maintained at approximately 10^{-9} Torr. Based on the Si peak intensities, the coverage and the thickness of the silane films on Al_2O_3

were determined to be uniform regardless of the receptor ($—NH_2$) density. Based on the relative peak intensity of N1s and Si2p peaks, the surface composition was determined [9].

2.7. SEM Analysis

The fracture surfaces from the T-peel tests were characterized using scanning electron microscopy (SEM). SEM micrographs of the fracture surfaces were obtained with a JEOL 940 microscope operated at 5 kV. The fractured polymer surfaces were sputtered with gold under 25 mA for 1 min.

3. RESULTS AND DISCUSSION

3.1. Model Substrate: Self-assembly of Mixed AS and MS

Figure 4 shows the experimental results of the solution mole fraction *vs.* the surface mole fraction determined by XPS analysis, where the total combined concentrations remained constant. The results were fitted using a competitive adsorption model, which is discussed below.

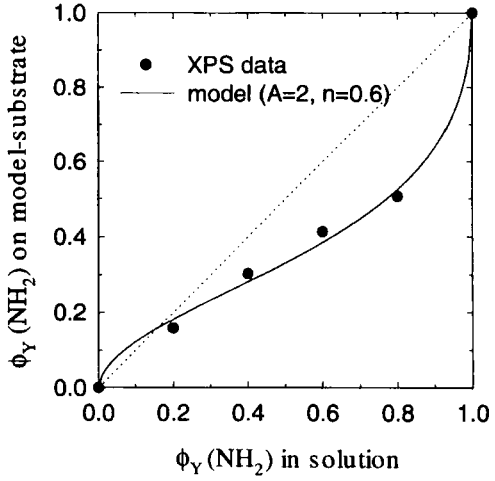

FIGURE 4 Competitive coadsorption of AS and MS in solution onto Al_2O_3.

The formation of mixed silane layers with AS and MS is dominated by kinetic effects associated with hydroxyl groups on the aluminum surface [17]. This resulted in the irreversible formation of silicon–oxygen bonds with strengths of approximately 128 kcal/mol [19]. This factor was first addressed when studying mixed monolayer formation [20], and is equally applicable to our system where the adsorption reaction of the silanes to the Al surfaces is quite fast. The adsorption rate of each adsorbate can be expressed by

$$r_1^{\text{surf}} = \frac{dc_1^{\text{surf}}}{dt} = k_1' \, c_1^{\text{solu}} \tag{2}$$

$$r_2^{\text{surf}} = \frac{dc_2^{\text{surf}}}{dt} = k_2' \, c_2^{\text{solu}} \tag{3}$$

where r, surf, solu, and k represent adsorption rate, surface, solution, and reaction constant, respectively. The overall rate of silane layer formation is the sum of the incorporation rates of the individual adsorbates.

$$r_{\text{total}}^{\text{surf}} = \frac{dc_1^{\text{surf}} + dc_2^{\text{surf}}}{dt} = k_1' c_1^{\text{solu}} + k_2' \, c_2^{\text{solu}} \tag{4}$$

Thus,

$$\phi_2^{\text{surf}} = \frac{r_2^{\text{surf}}}{r_{\text{total}}^{\text{surf}}} = \frac{k_2' \, c_2^{\text{solu}}}{k_1' \, c_1^{\text{solu}} + k_2' \, c_2^{\text{solu}}} \tag{5}$$

$$\phi_2^{\text{surf}} = \frac{1}{\{(k_1'/k_2')(c_1/c_2) + 1\}^{\text{solu}}} \tag{6}$$

In the experiment, the concentrations, c_1 and c_2, remained constant and can be converted to solution fractions, ϕ(MS) and ϕ(AS). In addition, the adsorption reaction rates do not necessarily have a first-order dependence on the solution concentration, thus, a parameter, n, can be included in the above equation [21]. The competitive adsorption of AS and MS was analyzed using Eq. (7). The data were fitted to determine the model parameters A and n of this system, as shown in Figure 4.

$$\phi^{\text{surf}}(\text{NH}_2) = \phi(\text{AS})^{\text{surf}} = \frac{1}{\{A(\phi(\text{MS})/\phi(\text{AS}))^n + 1\}^{\text{solu}}} \quad (7)$$

where A is the ratio of apparent surface reaction constant, $k'_{\text{MS}}/k'_{\text{AS}}$. The first parameter A was determined to have a value of 2, which roughly means that MS adsorbed to Al_2O_3 twice as fast as AS. The second parameter n was determined to be 0.6, which means that the competitive adsorption reaction was negatively cooperative for AS. Mixed self-assembly is crucial in designing surfaces for biodetectors and in studying cell adhesion on biological substrates. In this work, model substrates formed by a self-assembly of AS and MS on Al_2O_3 were used to understand the fundamentals of substrate receptor group effects on polymer adhesion.

3.2. Contact Angle Analysis

The surface restructuring of cPBD resulting from the diffusion and adsorption of COOH groups to interfaces were examined using contact angle analysis. Figure 5 shows the results of the advancing contact angles of hexadecane, water, and methylene diiodide on a cPBD surface (2.8 mol % of COOH) in terms of contact time. The surface tensions of the probing liquids are 27.6, 72.6, and 50.8 dyne/cm at room temperature, respectively. Since sticker–receptor interaction strength at the molecular scale is more important than the surface

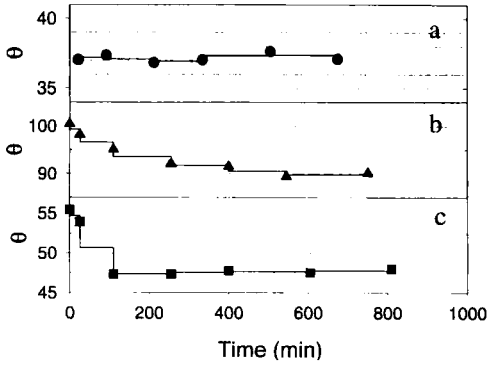

FIGURE 5 Contact angle (advancing) change of (a) hexadecane, (b) water, and (c) methylene diiodide on cPBD (2.8 mole % –COOH) with contact time.

tension of the probing liquid, the surface restructuring of cPBD cannot be simply related to the surface tensions of the probing liquids. The normalized contact angle, θ, *vs.* aging time of the cPBD-coated surfaces is shown in Figure 6. After the polymers are placed in contact with different media, the surface polymer chains restructure, depending on the enthalpic driving force of the media and the entropic constraint of the polymer. The thermodynamic adhesion energies between —COOH (sticker group) and $-CH_3$, —OH, and $-NH_2$ were reported to be less than 1 kcal/mol (van der Waals force), $3 \sim 5$ kcal/mol (hydrogen bond), and $16 \sim 25$ kcal/mol (strong acid–base interaction), respectively [22]. Since the hydrophilic COOH groups have a specific interaction (hydrogen bonding or acid–base interaction) with hydrophilic media, *e.g.*, water and methylene diiodide, there exists a driving force for surface movement and restructuring of the polymer/media surface. No contact angle change was observed with hydrophobic media, such as hexadecane. This was expected, since there was no extra driving force for the hydrophobic medium to move COOH to the surface. It was shown that the individual adhesion strength between polymer sticker groups and the medium functionality was more important than the surface tension of the probing liquid,

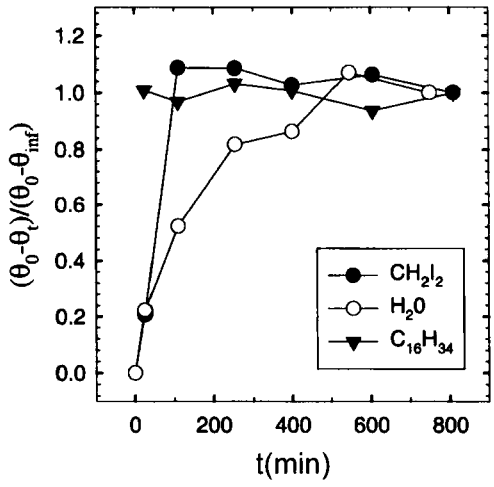

FIGURE 6 Normalized contact angle (advancing) change of various probing liquids on cPBD (2.8 mole % —COOH) with contact time.

because $-I_2$ groups caused faster restructuring of the cPBD surface (less than 100 min) than —OH groups (approximately 1000 min). It can be concluded from this result that the surface energetics of the substrate toward polymer sticker groups is closely related to the interfacial chain restructuring process. This interaction results in, the interesting G_{IC} adhesion kinetics discussed in the following section. The characteristic restructuring time of the bulk polymer chain was only of the order of one minute [9], but the contact angle changed in the experimental time scale was up to 1000 minutes. This indicates that the surface chain dynamics cannot be explained *via* the bulk chain dynamics such as reptation time, terminal relaxation time, and self-diffusion time.

As shown in Figure 7, the water advancing contact angle, $\theta_a(H_2O)$, of the substrates with the pure AS ($\phi_Y = 1$, total $-NH_2$) was measured to be 83.5° (± 1.5°) and with pure MS ($\phi_Y = 0$, total $-CO_3$) was 96.8° (± 3°). The contact angle for the untreated Al_2O_3 (total —OH) was approximately 43° (± 3°). When determining the contact angles of the model surfaces, the Al_2O_3 surfaces were used, regardless of the measurement of the contact angles of the cPBD surfaces. This is because the cPBD on the cover glass slide were multilayers, but the monolayer-like silane coatings were monolayers that did not perfectly

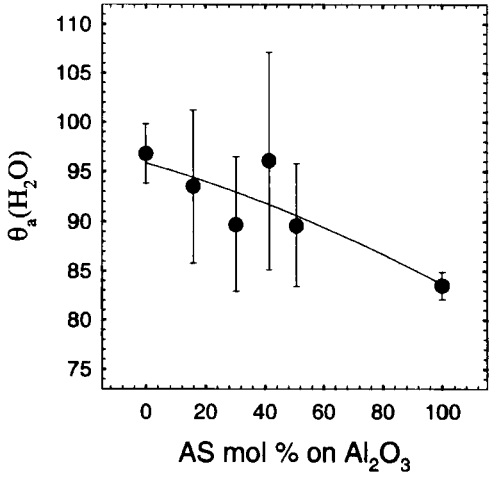

FIGURE 7 Contact angles (advancing) of water as a function of surface amine receptor density.

form two-dimensional monolayer films on Al_2O_3. No significant changes between AS- and MS-treated surfaces were observed. This is because other methylene groups of AS also interact with water molecules and the terminal $-NH_2$ groups of AS are apt to be contaminated by carbon-containing impurities, such as carbon dioxide and bicarbonates. The mixed silane monolayer-like coatings $0 < \phi_Y < 1$ showed large variations (6 to 11°) but gave θ_a values approximately along the linear interpolation line between the pure AS- and pure MS-coated substrates. Large variation of mixed monolayer-like silane coatings was normally shown in other mixed self-assembled systems [20]. From the literature [23], the $\theta_a(H_2O)$ of monolayer-like silane coatings were reported as 88.4° (± 4°) for an AS-treated surface. $\theta_a(H_2O)$ of the monolayer-like silane coatings varied with the length and the packing of carbon backbone chains, as well as the terminal functional groups [24]. The $\theta_a(H_2O)$ was reported as 102° (± 2°) for an *n*-butyltrichlorosilane-treated surface which has one more carbon chain (C4) relative to MS (C3), 62° to 76° for tert butyltrichlorosilane (C4) treated surfaces, and 112° (± 2°) for octadecyltrichlorosilane (C18) treated surfaces.

3.3. Fracture Energy of the Model Polymer–Solid Interfaces

3.3.1. Sticker Concentration $\phi(X)$ Effect

The fracture energy, G_{IC}, of the weak interface, the pure PBD–Al and the pure PBD–AlS interfaces, was determined to be approximately 10 J/m^2 at all annealing times regardless of the substrate receptor group density. The pure PBD surfaces interacted with the model substrate by van der Waals forces. When a few percent of sticker groups was introduced onto the pure PBD through a high-pressure carboxylation reaction, G_{IC} changed remarkably with the polymer sticker concentration, as shown in Figure 2. Figure 2 shows the effect of polymer sticker group concentration (0 to 7 mole % —COOH), $\phi(X)$, at constant $\phi(Y)$, on the fracture energy, G_{IC} [10]. It was shown that a critical concentration of sticker groups, approximately 3 mole % COOH, gave the optimal chain connectivity near the surface that caused the maximum fracture energy, 300 J/m^2. A carboxylated

polybutadiene (cPBD)–Al_2O_3 substrate system was used to show that the cohesive strength, G_{IC}, of the copolymer was improved with increasing sticker groups up to an optimal sticker concentration, after which G_{IC} decreased due to the dense attachment to the solid.

3.3.2. Receptor Concentration $\phi(Y)$ Effect

When the receptor concentration was varied (0 to 100 mol % $-NH_2$), G_{IC} changed remarkably with the substrate receptor concentration. Figure 8 shows that G_{IC} increases with increasing receptor concentration up to the critical point $\phi_Y^c \cong 30$ mol % coverage and then decreases with further increase in the receptor coverage for the long annealing time (1000 min). The maximum G_{IC} of 600 J/m^2 was almost the same value as the bulk cohesive G_{IC} of PBD [24]. However, at short time, G_{IC} increased as the density of substrate receptor group increased, as was expected. The fracture energy of the polymer–solid interface is determined by the weaker of the adhesive strength and cohesive strength. When the receptor density and annealing time are small, increasing the receptor group concentration increases the

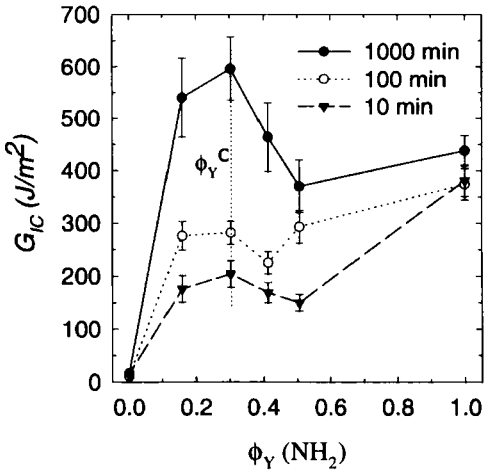

FIGURE 8 Substrate receptor concentration effect on the fracture energy of cPBD–AlS interfaces at various annealing times in which the sticker concentration was the same (approximately 3 mole % —COOH) and the peeling rate was 30 mm/min. The data point at $\phi_Y(NH_2) = 0$ is based on the purely dispersive force of PBD [9].

adhesive strength. However, at high concentration and at long annealing times, the dense attachment of the near-surface layer to the solid substrate caused a decrease in the cohesive strength, as the receptor density increased [9].

3.3.3. Adhesion Kinetics

No specific annealing time dependence of G_{IC} is shown for the samples made from the pure PBD, while strong annealing time dependence is shown for the cPBD–AlS interfaces, in the experimental time scale of 10–1000 min. The fracture energy did not change much with further annealing to 2000 min.

In Figure 8 the two characteristic cases of the G_{IC} of cPBD–AlS interfaces can be compared. The low energetic surface, $\phi(Y) \sim 0.3$, showed more than two orders of magnitude longer time dependence of G_{IC} than the high energetic surface, $\phi(Y) \sim 1.0$. Also, the restructuring time of cPBD at the polymer–solid interface (up to 1000 min) was much longer than the characteristic time of the bulk chain (~ 1 min). The longer restructuring time resulted from the change of the chain dynamics from the snake-like reptation motion of linear chain polymers to the star-arm like retraction motion near the polymer–solid interface. The restructuring time near the interface could be very long, due to its exponential dependence on the molecular weight and the hindered motion in the presence of the solid wall. The results of the time dependence of G_{IC} depending on the surface energetics were qualitatively the same with the results from the DCA analysis depending on the probing solvents, as explained in Section 3.2.

The adhesion kinetic analysis was further confirmed SEM of the fracture surfaces by T-peel tests, as shown in Figure 9. At high density $\phi(Y) \sim 1$, the cPBD surface was very quickly perturbed, indicating rapid bonding at the polymer–solid interface. At low density, $\phi(Y) \sim 0.3$, the surface of cPBD was hardly perturbed at short time but it was much more perturbed when the system came closer to equilibrium. After the T-peel test was performed, the aluminum sides of the samples had polymer segments on the surface, indicating partial cohesive fracture. The interfacial fracture loci, as shown in Figure 10, were estimated from weight gain of the polymer segment on aluminum after fracture. The polymer segment on aluminum was burned off, and

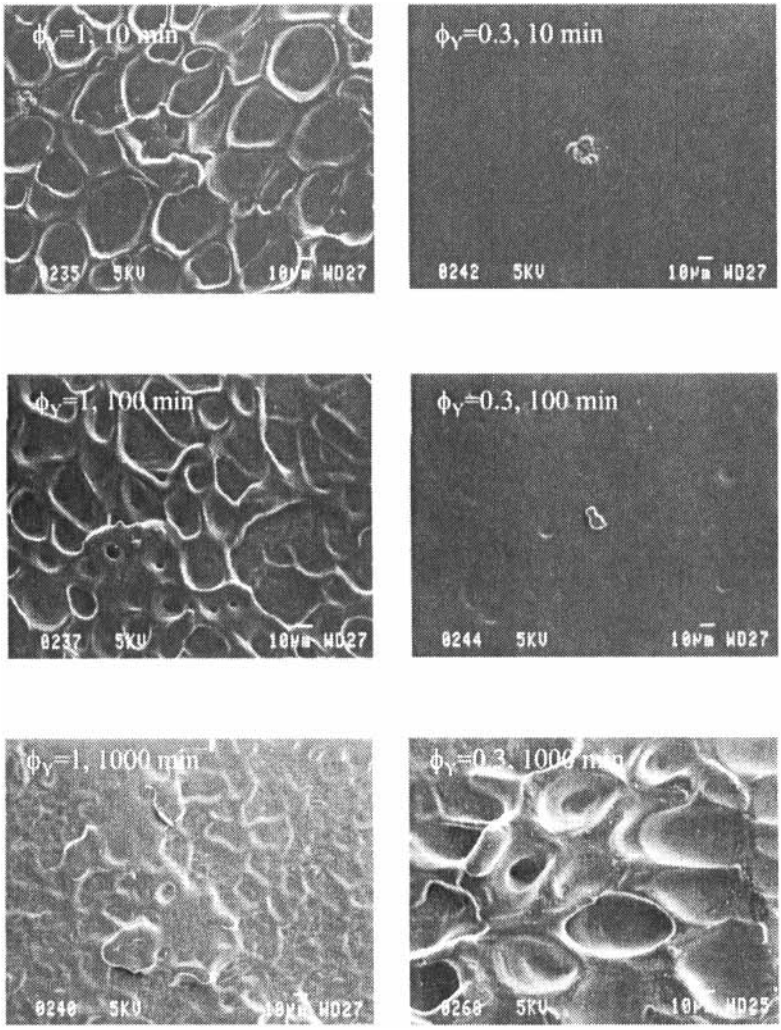

FIGURE 9 SEM micrographs of the fractured polymer surfaces at various annealing times.

the weight loss was converted to the average fracture locus based on polymer density. This result is similar in behavior to that of G_{IC}.

The schematic bonding dynamics of the two cases are shown in Figure 11. At high density, many active sites drive fast interactions with the sticker groups of the polymers but may prevent the chains

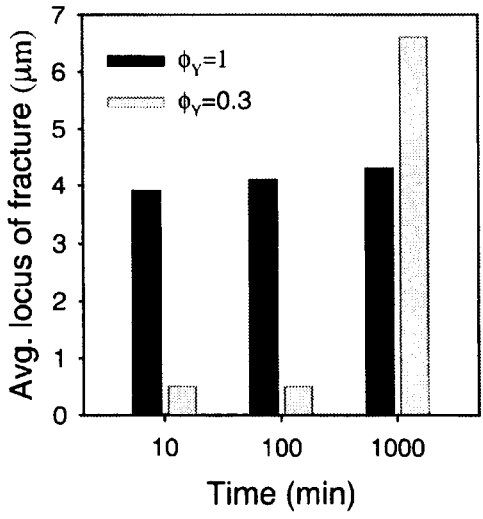

FIGURE 10 Average locus of failure determined by the weight gain of polymer segment on the solid surface after the fracture. One of the three tested samples at each annealing time was used.

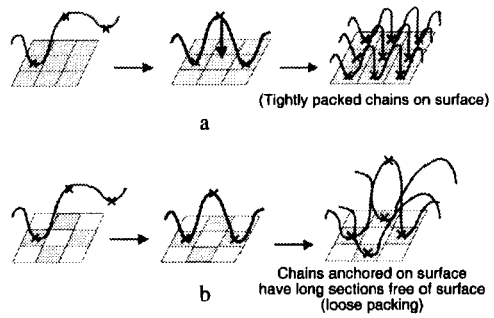

FIGURE 11 Schematic representation of bonding dynamics at the interface. (a) $\phi_Y = 1$, fast developing: facile motion (*e.g.*, chain excursion), (b) $\phi_Y = \phi_Y^c < 1$, slow developing: toilsome chain motion (*e.g.*, lateral movement to active site, initially in contact with non-active site).

from having the optimal chain conformation. Available active sites on the solids not yet occupied are apt to be taken by the other sticker groups of the same or other anchored chains rather than by those of free chains in the bulk. There are many strong and available active sites, enough to overcome the entropic constraints to some extent.

Near the optimum density, the free chains in the bulk can more easily find the available active sites on the solid than the anchored chains. These anchored chains have significant entropic constraint to their motion and, thus, to their ability to find available active sites. However, it takes much more time for the bulk chains to move and find active sites. At the interface, the grafted chains could be stretched away from the surfaces; and, thus, they will pack efficiently with the free chains.

3.3.4. *Influence of Peeling Rate and Annealing Temperature*

The interface fracture energy, G_{IC}, measured for polymers above their glass transition temperatures can be very high due to viscoelastic losses in the polymer layer [25]. Even though the intrinsic interface strength, G_0, remains approximately constant [26, 27], variations of several decades in G_{IC} are normally observed for polymers by changing the deformation rate, R, and temperature, T. The classic equation of interface failure is given empirically by [27].

$$G_{IC} = G_0[1 + f(R, T)] \tag{8}$$

where G_0 is the intrinsic fracture energy at zero rate, and $f(R, T)$ represents the dissipation contribution from the bulk polymers [28]. This equation predicts that a stronger interface (high G_0) allows higher stress transfer to the adhesive, causing enhanced energy dissipation in the adhesive layer [27, 29]. However, if the polymer–solid interface is too strong, the interface may not be efficient for transferring a high stress to the bulk adhesive, which is the main point of this paper. For the weak interface governed by purely dispersive (van der Waals) forces, G_0 is the thermodynamic work of adhesion, W_A [26, 27] [$G_0 \cong W_A \cong 0.1\,J/m^2$]. Andrews and Kinloch [27] effectively normalized out the huge contribution of viscoelastic dissipation in the adhesive [$1 + f(R, T)$], leaving a G_0 term ($W_A = 0.07\,J/m^2$) with a model polymer on inert substrates, where only dispersive interactions exist across the interface. For strong interfaces, dominated by chemical bonding across the interface, the values of G_0 at reduced rates become much higher than W_A [25]. It was expected that specific bonding, like

hydrogen bonding or acid–base interactions, in some systems would contribute to values of G_0 somewhat greater than W_A [25].

Figure 12 shows the G_{IC} *vs.* peeling rate, R_p, and annealing temperature dependencies for the cPBD–AlS interface with $\phi(Y) = 1$. The cPBD–AlS interface was fully developed up to 2 days before the test. The interface failure Eq. (8) was investigated by using $G_{IC} = G_0(1 + aR_p^n)$. The results were fitted using Jandel Sigma Plot software with experimental data in the experimental R_p scale of 0.6–190 mm/min.

$$G_{IC} = 5.4[1 + 47R_p^{0.15}] \quad \text{annealed at } 23°C \tag{9}$$

$$G_{IC} = 4.9[1 + 54R_p^{0.12}] \quad \text{annealed at } 70°C \tag{10}$$

Specimens showed a relatively low peeling rate dependence of the exponent of 0.12–0.15 in the experimental peeling rate scale. It was reported for the polydimethylsiloxane case that in the non-Newtonian region, $R_p > R_p^*$, the data behaved approximately as $G_{IC} \sim R_p^{0.14}$, where R_p^* is a film thickness divided by a reptation time, T_r [30]. In our system, T_r and R_p^* were determined to be 1.6 sec and 0.6 mm/min, respectively [9]. At the elevated annealing temperature (70°C) and under vacuum it was observed that the cPBD started cross-linking. The cPBD annealed at 70°C under vacuum did not dissolve in solvent,

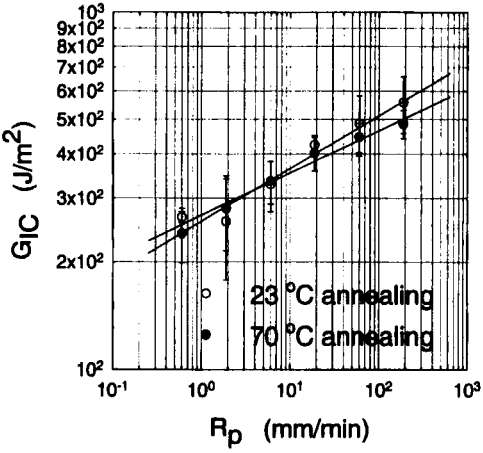

FIGURE 12 Peeling rate and annealing temperature effects on the fracture energy.

THF, while the cPBD annealed at room temperature dissolved in THF. The master curve of cPBD using the time-temperature superposition was not performed because of cross-linking. Although it was difficult to quantify because of the level of experimental error, it appeared that the cross-linking of the adhesive layer may have prevented the interfacial chains from forming an efficient structure which would decrease the dissipation of the observed G_{IC} at high R_p. It is known that the dissipating energy term dominates the observed peel energy over the energy to break the C—C bond [30]. However, due to the limited range of peeling rate in this work, it was not clear whether G_0 determined by data fitting was the intrinsic fracture energy.

4. OPTIMUM PBD ADHESION AT POLYMER–SOLID INTERFACE

The enthalpic adsorption energy, ΔH, of the chain can be related to the gain of intrinsic adhesive strength, G_A, between an adsorbed chain and a solid surface. Simultaneously, the entropy loss, ΔS, of an adsorbed chain collapsing to the attractive surface can be related to the decrease of intrinsic cohesive failure energy, G_C, between an adsorbed chain and other neighboring chains. At equilibrium, the ΔS decrease of an adsorbed chain critically depends on the gain in ΔH. Thus, G_A and G_C are not independent of each other, but they move in opposite directions as the surface energetics increases, as illustrated in Figure 13. The polymer sticker groups and the substrate receptor

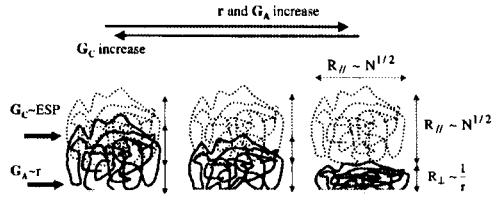

FIGURE 13 Schematic representations of the conformational dimension of an adsorbed chain on a solid surface and the two adhesion potentials, the adhesive potential between an adsorbed chain and a solid surface (G_A) and the cohesive potential between an adsorbed chain and neighboring free chains (G_C). They move in opposite directions as r increases at the interface.

TABLE I Summary of the experimental results of the effects of PBD and Al_2O_3 surface modifications on G_{IC}. Further details of the cases 1, 2 and 3 can be seen in Refs. [10, 31 and 9], respectively

Case	$\chi(X-Y)$ (*cal/mol*)	*Optimum* $\phi^*(X)$ *or* $\phi^*(Y)$	*Optimum* r^* $[\chi\phi(X)\ \phi(Y)]^*$ (*cal/mol*)	*Maximum* G_{IC}^* (J/m^2)
1. cPBD–Al	$3000 \sim 5000$ (—COOH *vs.* —OH)	$\phi^*(X) = 3$ mol % at constant $\phi(Y)$ ($= 100$ mol %)	$90 \sim 150$	300 ± 25
2. cPBD–AlS	$16000 \sim 25000$ (—COOH *vs.* —NH_2)	$\phi^*(X) = 0.5$ mol% at constant $\phi(Y)$ ($= 100$ mol %)	$80 \sim 125$	600 ± 50
3. cPBD–AlS	$16000 \sim 25000$ (—COOH *vs.* —NH_2)	$\phi^*(Y) = 30$ mol% at constant $\phi(X)$ ($= 3$ mol %)	$144 \sim 225$	600 ± 60

groups changed the enthalpic driving force and, thus, entropic constraints, at the polymer–solid interface, which resulted in the interesting G_{IC} variation as a function of sticker groups and receptor groups [9, 10]. If $\chi\phi_X\phi_Y$ varies only within very low or very high regions, we can not expect the cross-over point of the two interface potentials, without observing a maximum fracture energy of a polymer–solid interface strength. In this work, we used modified polybutadiene and modified surfaces to prepare a wide range of $\chi\phi_X\phi_Y$ and we observed the maximum G_{IC} at an optimum product value of $\chi\phi_X\phi_Y$, as summarized in Table I. Again, it can be qualitatively explained that when $\chi\phi_X\phi_Y$ is small, increasing the sticker group and receptor group concentrations increases the adhesive strength. However, at high concentrations, the dense attachment of the near-surface layer to the solid substrate decreases the cohesive strength. The fracture energy of a polymer–solid interface is subject to the weaker of the adhesive strength and cohesive strength. The cPBD–Al interface showed an optimum G_{IC} of 300 J/m^2, but cPBD–AlS interfaces showed an optimum G_{IC} of 600 J/m^2 that is almost equivalent to the bulk cohesive value of PBD [24]. This is because the silane layer in cPBD–AlS interfaces (Cases 2 and 3 in Tab. I) acted as a primer to cause more efficient dissipation processes than in cPBD–Al interfaces (Case 1 in Tab. I). Interestingly, we found that there existed an optimum product value, $r^* = (\chi\phi_X\phi_Y)$, of approximately 150 cal/mol, when we used χ as the real interaction strength rather than the normalized parameter, which resulted in maximum G_{IC} for our model polymer–solid interfaces. Consequences and further interpretation of the optimal interface structure expressed through r^* are discussed elsewhere [18].

5. CONCLUSION

The design criteria for making strong polymer–solid interfaces were studied using model polymer–solid interfaces: carboxylated polybutadiene adhered to mixed silane modified aluminum surfaces, where the sticker concentration, the receptor concentration, and the sticker–receptor pairs were varied over a wide range. Some important effects

of such variables on polymer adhesion were found:

(1) Appropriate annealing times required for polymer adhesion were found to be much longer (up to 1000 min) than the characteristic time of a bulk chain (less than 1 min), such as reptation time, terminal relaxation time, and self diffusion time. The contact angles of various probing liquids on the model polymer and the fracture energy of the model polymer–solid interfaces varied with the contact time, which showed longer time dependence than the characteristic time of a bulk polymer chain and was a function of enthalpic driving forces between the model polymer and the media.

(2) Small amounts of polymer sticker groups randomly distributed along the polymer backbone chain abruptly increased the fracture energy of the weak polymer–solid interface by $2 \sim 3$ orders of magnitude (from less than $10\,J/m^2$ up to $600\,J/m^2$). The fracture energy was not a monotonic function of the polymer sticker concentration. After the critical sticker concentration, the fracture energy decreased with further addition of stickers.

(3) Amine-terminated silane monolayer-like coatings on aluminum oxide surfaces doubled the maximum fracture energy of the model polymer–metal interfaces, from $300\,J/m^2$ to $600\,J/m^2$. This is because the silane layer acted as a primer between the model polymer and the solid surface, resulting in efficient stress transfer through the interface. Here, the fracture energy was not a monotonic function of the polymer–receptor concentration at long annealing time (1000 min). After the critical receptor concentration (30 mol % $-NH_2$), the fracture energy decreased with increasing receptors. However, at short annealing time (10 min), the fracture energy approximately corresponded to the receptor concentration. At intermediate annealing time (100 min), the fracture energy showed no receptor density effect.

(4) Changes in sticker concentration, receptor concentration, and sticker–receptor pair at the interface show critical sticker and receptor concentration, resulting in maximum fracture energy. These critical concentrations shifted to the left or right depending on the sticker-receptor interaction strength, but the product value of the sticker concentration, the receptor concentration, and the

interaction strength remained approximately the same, about 150 cal/mol for polybutadiene adhesion.

(5) Classical design criteria failed to explain the effect of sticker–receptor interactions on polymer adhesion: The fracture energy of polymer–solid interfaces was not a monotonic function of the sticker–receptor interactions. This is because the adhesive potential between adsorbed chains and a solid surface and the cohesive potential between adsorbed chains and neighboring chains move in opposite directions, as the number of interactions increases. The failure occurs at the weaker of the two potentials that always exist at polymer–solid interfaces.

In summary, through experiments and the modified scaling theory, it was found that optimum product value of sticker concentration, receptor concentration, and their interaction parameter exists to maximize the adhesion strength of polymer–solid interfaces. Below this optimum product value, the G_{IC} increased with an increase in any of these parameters, and after the optimum product value, G_{IC} decreased with an increase in any of the parameters.

Acknowledgement

This work was funded by Hercules, Inc., Wilmington, Delaware and NSF through grant DMR 9596-267.

References

[1] Subramanian, S. and Lee, S., *Polym. Eng. Sci.* **39**(11), 2274–2281 (1999).
[2] Lee, Y. and Char, K., *Macromolecules* **31**, 7091–7094 (1998).
[3] Cho, K. W., Seo, K. H., Ahn, T. O., Kim, J. and Kim, K. U., *Polymer* **38**, 4825–4830 (1997).
[4] Tan, B. N. C., Peiffer, D. G. and Briber, R. M., *Macromolecules* **29**, 4969–4975 (1996).
[5] Cho, C. K., Cho, K. and Park, C. E., *J. Adhesion Sci. Technol.* **11**, 433–445 (1997).
[6] In: *Polymer Surface Modification: Relevance to Adhesion*, M. Strobel *et al.* Eds. (VSP, Utrecht, The Netherlands, 1996).
[7] Stralin, A. and Hjertberg, T., *Surf. Interface Anal.* **20**, 337–340 (1993).
[8] Inagaki, N., Tasaka, S., Narushima, K. and Mochizuki, K., *Macromolecules* **32**, 8566–8571 (1999).
[9] Lee, I. and Wool, R. P., *Macromolecules* **33**, 2680–2687 (2000).
[10] Gong, L. Z., Friend, A. D. and Wool, R. P., *Macromolecules* **31**, 3706–3714 (1998).

[11] Léger, L., Raphäel, E. and Hervet, H., *Advances in Polymer Science* **138**, 185–225 (1999).
[12] Creton, C., Brown, H. R. and Deline, V. R., *Macromolecules* **27**, 1774–1780 (1994).
[13] Guiselin, O., *Europhys. Lett.* **17**, 225–230 (1992).
[14] O'Connor, K. and McLeish, T., *Faraday Discuss.* **98**, 67–78 (1994).
[15] Fowkes, F. M. and Mostafa, M. A., *Ind. Eng. Chem. Prod. Res. Dev.* **17**, 3–7 (1978).
[16] Gong, L. Z., Wool, R. P., Friend, A. D. and Konstantin, G. J., *J. Polym. Sci. Polym. Chem.* **37**, 3129–3138 (1999).
[17] Plueddemann, E., *Silane Coupling Agents* (Plenum, New York, 1982).
[18] Lee, I., *Ph.D. Dissertation* (University of Delaware, Newark, Delaware, 2000).
[19] Walsh, R., *Acc. Chem. Res.* **14**, 246–252 (1981).
[20] Folker, J. P., Laibinis, P. E. and Whitesides, G. M., *Langmuir* **8**, 1330–1341 (1992).
[21] Offord, D. A. and Griffin, J. H., *Langmuir* **9**, 3015–3025 (1993).
[22] Thomas, R. C., Houston, J. E., Crooks, R. M., Kim, T. and Michalske, T. A., *J. Am. Chem. Soc.* **117**, 3830–3834.
[23] Harding, P. H. and Berg, J. C., *J. Appl. Polym. Sci.* **67**, 1025–1033 (1988).
[24] Roland, C. M. and Bohm, G. G. A., *Macromolecules* **18**, 1310–1314 (1985).
[25] Sauer, B. B., Bochanour, C. R. and Van Alsten, J. G., *Macromolecules* **32**, 2739–2747 (1999).
[26] Gent, A. N. and Hamed, G. R., *Proc. R. Soc. London A* **310**, 433 (1969).
[27] Andrews, E. H. and Kinloch, A. J., *Proc. R. Soc. London A* **332**, 385 (1973).
[28] Gent, A. N. and Hamed, G. R., *Plastics Rubber Proc.* **3**, 17 (1978).
[29] Brown, H. R., *Annu. Rev. Mater. Sci.* **21**, 463–489 (1991).
[30] Wool, R. P., *Polymer Interface: Structure and Strength* (Hanser/Gardner, New York, 1995).
[31] Gong, L. Z. and Wool, R. P., *J. Adhesion* **71**, 189–209 (1999).